

# Theoretical equations of state for temperature and electromagnetic field dependence of fluid systems, based on the quasi-Gaussian entropy theory

A. Amadei<sup>a)</sup>

*Department of Chemical Sciences and Technology, University of Rome "Tor Vergata," Via della Ricerca Scientifica 1, 00133, Rome, Italy*

M. E. F. Apol

*Department of Chemistry, University of Rome "La Sapienza," P. le A. Moro 5, 00185, Rome, Italy  
and Department of Biophysical Chemistry, University of Groningen, Nijenborgh 4, 9747 AG Groningen, The Netherlands*

G. Brancato and A. Di Nola

*Department of Chemistry, University of Rome "La Sapienza," P. le A. Moro 5, 00185, Rome, Italy*

(Received 2 May 2001; accepted 11 December 2001)

The quasi-Gaussian entropy (QGE) theory employs the fact that a free-energy change can be written as the moment-generating function of the appropriate probability distribution function of macroscopic fluctuations of an extensive property. By modeling this distribution, one obtains a model of free energy and resulting thermodynamics as a function of one state variable. In this paper the QGE theory has been extended towards theoretical models or equations of state (EOS's) of the thermodynamics of semiclassical systems as a function of two state variables. Two "monovariate" QGE models are combined in the canonical ensemble: one based on fluctuations of the excess energy (the confined gamma state giving the temperature dependence) and the other based on fluctuations of the reduced electromagnetic moment [various models as derived in the preceding paper [Apol, Amadei, and Di Nola, *J. Chem. Phys.* **116**, 4426 (2002)], giving the external field dependence]. This provides theoretical EOS's for fluid systems as a function of both temperature and electromagnetic field. Special limits of these EOS's are considered: the general weak-field EOS and the limit to a Curie's law behavior. Based on experimental data of water and simulation data using the extended simple point charge (SPC/E) water model at 45.0 and 55.51 mol/dm<sup>3</sup>, the specific EOS based on a relatively simple combination of the confined gamma state model with a discrete uniform state field model accurately reproduces the dielectric properties of water at constant density, as the temperature dependence of the weak-field dielectric constant for gases and liquids, and the field dependence of the dielectric constant of liquids. © 2002 American Institute of Physics. [DOI: 10.1063/1.1448291]

## I. INTRODUCTION

The development of reliable and relatively workable equations of state (EOS's) for real systems, based on statistical mechanics, is still a challenging problem in chemistry and physics. Many successful and unsuccessful attempts have been made to derive general theoretical descriptions for the statistical mechanics and thermodynamics as a function of one or more state variables, e.g., temperature ( $T$ ), pressure ( $p$ ), volume ( $V$ ), etc. Examples of EOS's that depend only on one state variable are "thermal" ( $T$ ) and "mechanical" ( $V$ ) equations of state. One of the statistical-mechanical approaches towards such general "monovariate" EOS's is the quasi-Gaussian entropy (QGE) theory.

So far the QGE theory provided theoretical models for the thermodynamics as a function of temperature,<sup>1-4</sup> density,<sup>5</sup> pressure,<sup>5</sup> and external field,<sup>6</sup> by modeling the dis-

tributions of appropriate macroscopic fluctuations by "quasi-Gaussian" distributions, i.e., via the convolution of distributions corresponding to identical and statistically independent subsystems.<sup>1,6</sup> Application of the QGE theory to many different systems showed that relatively simple models can describe with high accuracy the thermodynamics of both solids<sup>3</sup> and fluids.<sup>1,4,7,8</sup>

In this paper we will illustrate how the QGE theory can be extended towards theoretical models that describe the thermodynamics as a function of two state variables ("bivariate" models). Such bivariate equations of state are implicitly based on specific assumptions on the underlying bivariate distribution of fluctuations of two macroscopic properties, e.g., excess energy and volume, or excess energy and the electromagnetic moment. In this paper, however, we do not use any direct modeling of such a bivariate distribution, but instead use a specific combination of two monovariate QGE models. In this case we present the combination of fluctuations of the excess energy and the electromagnetic moment in the canonical ensemble, to derive theoretical

<sup>a)</sup>Author to whom correspondence should be addressed. Electronic mail: andrea.amadei@uniroma2.it

equations of state that provide the thermodynamics of fluid systems at fixed density as a function of both temperature and electromagnetic field.

An EOS, based on a specific combination of a confined gamma state for the excess energy fluctuations with a discrete uniform state for fluctuations of the electromagnetic moment, will be tested on (experimental and simulated) data of fluid water.

## II. THEORY

### A. Basic definitions and derivations

In this article we will use the same general notation of electromagnetic (em) properties as in Ref. 6 (hereafter referred to as I). For an ellipsoidal system containing  $N$  molecules at temperature  $T$  and volume  $V$ , with a homogeneous external electromagnetic field  $\mathfrak{F}_0$  aligned along one of the ellipsoidal axes, the canonical partition function is given by<sup>6</sup>

$$Q = \sum_n e^{-\beta[\mathcal{E}_n^{(0)} - \mathcal{M}'_n \mathfrak{F}_0 + \frac{1}{2} \mathcal{A} \mathfrak{F}_0^2]}, \quad (1)$$

where  $\mathcal{E}_n^{(0)}$  is the unperturbed energy of the  $n$ th quantum state without external field.  $\mathcal{M}_n = \mathcal{M}'_n - \mathcal{A} \mathfrak{F}_0$  is the total em moment in the direction of the field, and  $\beta = 1/kT$ . Within the approximation used in I,  $\mathcal{A}$  is a pure constant, independent of field and temperature. In the Appendix an explicit expression of  $\mathcal{A}$  in terms of susceptibility is derived. We exclude systems that exhibit hysteresis effects.

Since in the present paper we are interested in the properties of fluids, we can take the most general expression for the semiclassical limit of  $Q$ , giving<sup>1,9</sup>

$$\begin{aligned} Q &= \frac{1}{N! h^d (1 + \gamma)^N} \sum_i \int^* e^{-\beta \mathcal{U}_i} d\boldsymbol{\xi} d\boldsymbol{\pi} \\ &= \frac{(2\pi kT)^{d/2}}{N! h^d (1 + \gamma)^N} \sum_i \int^* e^{-\beta[\Phi + \Psi + \mathcal{E}_i + \mathcal{M}'_i \mathfrak{F}_0 + \frac{1}{2} \mathcal{A} \mathfrak{F}_0^2]} \\ &\quad \times \prod_{j=1}^N (\det \tilde{M}_j)^{1/2} d\boldsymbol{\xi}, \end{aligned} \quad (2)$$

where  $\mathcal{U}$  is the Hamiltonian of the system, which is a function of the generalized coordinates  $\boldsymbol{\xi}$  and their conjugated momenta  $\boldsymbol{\pi}$ , and the star on the integrals denotes as usual that we integrate only in the accessible part of configurational space.<sup>1</sup> All symbols have their usual meaning:<sup>1,9</sup>  $\Phi$  and  $\Psi$  are the classical intermolecular and intramolecular potential energy, and  $\mathcal{E}_i$  is the possible quantum-mechanical vibrational energy of the bond lengths and angles.  $\det \tilde{M}_j$  is the determinant of the mass tensor of the  $j$ th molecule,  $d$  is the total number of classical degrees of freedom,  $h$  is the Planck constant, and  $(1 + \gamma)$  the symmetry coefficient per molecule.<sup>10,11</sup> The electronic energy is considered to be completely confined within the ground state. Moreover,  $\mathcal{M}'_i$  now depends on the coordinates and in principle on the quantum vibrational state.<sup>12</sup>

Similarly to what was done in a previous paper for systems without an external field [cf. Eq. (5) of Ref. 1], we can

use a rather general approximation to simplify Eq. (2). Assuming that, at least for most of the quantum states,

$$\begin{aligned} &\int^* e^{-\beta[\Phi + \Psi + \mathcal{E}_i - \langle \mathcal{E}_i \rangle - (\mathcal{M}'_i - \langle \mathcal{M}'_i \rangle) \mathfrak{F}_0]} \prod_{j=1}^N (\det \tilde{M}_j)^{1/2} d\boldsymbol{\xi} \\ &\cong \int^* e^{-\beta[\Phi + \Psi + \mathcal{E}_0 - \langle \mathcal{E}_0 \rangle - (\mathcal{M}'_0 - \langle \mathcal{M}'_0 \rangle) \mathfrak{F}_0]} \prod_{j=1}^N (\det \tilde{M}_j)^{1/2} d\boldsymbol{\xi}, \end{aligned} \quad (3)$$

where  $\langle \mathcal{E}_i \rangle$  and  $\langle \mathcal{M}'_i \rangle$  are the coordinate-averaged values in the  $i$ th quantum state, with the zero subscript indicating the ground-state properties, we obtain

$$\begin{aligned} &\sum_i \int^* e^{-\beta[\Phi + \Psi + \mathcal{E}_i - \mathcal{M}'_i \mathfrak{F}_0 + \frac{1}{2} \mathcal{A} \mathfrak{F}_0^2]} \prod_{j=1}^N (\det \tilde{M}_j)^{1/2} d\boldsymbol{\xi} \\ &\cong \left( \sum_i e^{-\beta[\langle \mathcal{E}_i \rangle - \langle \mathcal{E}_0 \rangle - (\langle \mathcal{M}'_i \rangle - \langle \mathcal{M}'_0 \rangle) \mathfrak{F}_0 + \frac{1}{2} \mathcal{A} \mathfrak{F}_0^2]} \right) \\ &\quad \times \int^* e^{-\beta[\Phi + \Psi + \mathcal{E}_0 - \mathcal{M}'_0 \mathfrak{F}_0]} \prod_{j=1}^N (\det \tilde{M}_j)^{1/2} d\boldsymbol{\xi}. \end{aligned} \quad (4)$$

Furthermore, introducing the abbreviation

$$\begin{aligned} Q_{\text{ref}}^{\text{qm}} &= e^{-\beta[\mathcal{E}_{\text{ref},0} - \mathcal{M}'_{\text{ref},0} \mathfrak{F}_0 + \frac{1}{2} \mathcal{A} \mathfrak{F}_0^2]} \\ &\quad \times \sum_i e^{-\beta[\langle \mathcal{E}_i \rangle - \langle \mathcal{E}_0 \rangle - (\langle \mathcal{M}'_i \rangle - \langle \mathcal{M}'_0 \rangle) \mathfrak{F}_0]}, \end{aligned} \quad (5)$$

with  $\mathcal{E}_{\text{ref},0}$  and  $\mathcal{M}'_{\text{ref},0}$  some reference ground-state vibrational energy and em “moment,” both independent of the coordinates, the partition function can be written as

$$\begin{aligned} Q &= \frac{(2\pi kT)^{d/2} Q_{\text{ref}}^{\text{qm}}}{N! h^d (1 + \gamma)^N} \int^* e^{-\beta[\Phi + \Psi + \mathcal{E}_0 - \mathcal{E}_{\text{ref},0} - (\mathcal{M}'_0 - \mathcal{M}'_{\text{ref},0}) \mathfrak{F}_0]} \\ &\quad \times \prod_{j=1}^N (\det \tilde{M}_j)^{1/2} d\boldsymbol{\xi}. \end{aligned} \quad (6)$$

Note that in general  $\mathcal{M}'_{\text{ref},0}$  can be set to zero without reducing the generality of the expressions, and that  $Q_{\text{ref}}^{\text{qm}}$  reduces in the absence of an external field and for semirigid molecules to the ideal-gas vibrational partition function.<sup>1</sup>

If we define a reference state of the system with corresponding partition function

$$Q_{\text{ref}} = \frac{(2\pi kT)^{d/2} Q_{\text{ref}}^{\text{qm}}}{N! h^d (1 + \gamma)^N} \int \prod_{j=1}^N (\det \tilde{M}_j)^{1/2} d\boldsymbol{\xi}, \quad (7)$$

we readily obtain the ideal reduced (or excess) free energy<sup>1</sup>  $A'(T, \mathfrak{F}_0)$ :

$$\begin{aligned} A'(T, \mathfrak{F}_0) &\equiv A(T, \mathfrak{F}_0) - A_{\text{ref}}(T, \mathfrak{F}_0) \\ &= -kT \ln \left( \frac{\int^* e^{-\beta \mathcal{U}'} \prod_{j=1}^N (\det \tilde{M}_j)^{1/2} d\boldsymbol{\xi}}{\int^* \prod_{j=1}^N (\det \tilde{M}_j)^{1/2} d\boldsymbol{\xi}} \right) \\ &\quad - kT \ln \epsilon \\ &= kT \ln \langle e^{\beta \mathcal{U}'} \rangle - kT \ln \epsilon. \end{aligned} \quad (8)$$

Here  $\mathcal{U}'$  is the excess or ideal reduced (or, loosely speaking, “potential”) energy,

$$\mathcal{U}' = \Phi + \Psi + \mathcal{E}_0 - \mathcal{E}_{\text{ref},0} - (\mathcal{M}'_0 - \mathcal{M}'_{\text{ref},0})\mathfrak{F}_0 \quad (9)$$

and

$$\begin{aligned} \langle e^{\beta \mathcal{U}'} \rangle &= \frac{\int^* e^{-\beta \mathcal{U}'} e^{\beta \mathcal{U}'} \prod_{j=1}^N (\det \tilde{M}_j)^{1/2} d\xi}{\int^* e^{-\beta \mathcal{U}'} \prod_{j=1}^N (\det \tilde{M}_j)^{1/2} d\xi} \\ &= \int \rho(\mathcal{U}') e^{\beta \mathcal{U}'} d\mathcal{U}' \end{aligned} \quad (10)$$

is the moment generating function<sup>13,14</sup> of the probability density  $\rho(\mathcal{U}')$  of the excess energy  $\mathcal{U}'$ , which in the QGE theory is modeled as a “quasi-Gaussian” distribution, i.e., via the convolution of the distributions of identical and statistically independent subsystems. Finally,

$$\epsilon = \frac{\int^* \prod_{j=1}^N (\det \tilde{M}_j)^{1/2} d\xi}{\int \prod_{j=1}^N (\det \tilde{M}_j)^{1/2} d\xi} \quad (11)$$

is the fraction of phase space that is accessible to the system, due to, e.g., hard-body interactions.<sup>1</sup>

The free-energy change due to the field, at fixed temperature and density, is

$$\begin{aligned} \Delta A(T, \mathfrak{F}_0) &= A(T, \mathfrak{F}_0) - A(T, 0) \\ &= A'(T, \mathfrak{F}_0) - A'(T, 0) + A_{\text{ref}}(T, \mathfrak{F}_0) - A_{\text{ref}}(T, 0) \\ &= \Delta A'(T, \mathfrak{F}_0) + \Delta A_{\text{ref}}(T, \mathfrak{F}_0). \end{aligned} \quad (12)$$

In the case that  $\langle \mathcal{M}'_i \rangle \equiv \langle \mathcal{M}'_0 \rangle$ , i.e., if the electromagnetic moment is basically independent of the bond quantum vibrational state, and setting  $\mathcal{M}'_{\text{ref},0} = 0$ , we have

$$\Delta A_{\text{ref}}(T, \mathfrak{F}_0) = \Delta A_{\text{ref}}(\mathfrak{F}_0) = \frac{1}{2} \mathcal{A} \mathfrak{F}_0^2. \quad (13)$$

For simplicity, in this paper we will adopt such an assumption that proves to be a rather good approximation for the system studied. Hence, the free energy change  $\Delta A$ , the average em moment  $M = -\partial \Delta A / \partial \mathfrak{F}_0$  and its field derivative are related to the excess properties via

$$\Delta A(T, \mathfrak{F}_0) = \Delta A'(T, \mathfrak{F}_0) + \frac{1}{2} \mathcal{A} \mathfrak{F}_0^2, \quad (14)$$

$$M(T, \mathfrak{F}_0) = M'(T, \mathfrak{F}_0) - \mathcal{A} \mathfrak{F}_0, \quad (15)$$

$$\frac{\partial M(T, \mathfrak{F}_0)}{\partial \mathfrak{F}_0} = \frac{\partial M'(T, \mathfrak{F}_0)}{\partial \mathfrak{F}_0} - \mathcal{A}, \quad (16)$$

where  $M' = \langle \mathcal{M}' \rangle$  is the average reduced em moment.

## B. Construction of bivariate QGE models

In this section we show how two “monovariate” QGE models, one for the temperature and one for the field dependence, can be combined in the canonical ensemble to obtain a complete solution for the thermodynamics at fixed density as a function of temperature and field, a “bivariate” QGE model.

The two monovariate QGE models are the following. First, at fixed field and varying temperature, Eq. (8) provides the excess free energy as a function of (the moment gener-

ating function of) the distribution of the “potential” energy. Previously we have shown that at zero field a gamma distribution (yielding the confined gamma state) is an excellent model distribution for  $\rho(\mathcal{U}')$ , both for water<sup>1,4</sup> and the Lennard-Jones fluid.<sup>8</sup>

Second, from Eqs. (14) and (13) of I it follows that at fixed temperature  $T_0$  and varying field,

$$\Delta A'(T_0, \mathfrak{F}_0) = -kT \langle e^{\beta \mathcal{M}' \mathfrak{F}_0} \rangle_{\mathfrak{F}_0=0}. \quad (17)$$

Hence, the field dependence of the free energy is given by (the moment generating function of) the distribution of the reduced electromagnetic moment  $\mathcal{M}'$  at zero field. In I various models have been derived based on different (continuous and discrete) model distributions of  $\mathcal{M}'$ .

The theoretical equations of state we present in this paper are based on the following assumptions.

First, we assume that at least for one ellipsoidal geometry  $f_d$  the confined gamma state model is valid for describing the temperature dependence at any possible external field, aligned along one ellipsoidal axis. This confined gamma state is at zero field defined by the parameters  $U'_0$ ,  $C'_{V0}$ , and  $\delta_0$ .

Second, we assume that at one isotherm  $T_0$  we can use a given QGE model for the field dependence, as described in I.

The previous two assumptions are based on the great generality and accuracy of the gamma state model, at least at zero field, and of some of the models described in I. To proceed further, we must consider that we are interested essentially in weak- to medium-field conditions, as the high-field conditions are not only very difficult to be realized experimentally, but are also likely to determine relevant electronic rearrangements<sup>15,16</sup> and even chemical reactions that cannot be described by the present model based on second order perturbation expansion in the field; see I. This implies that in the field range of interest, simple first-order expansions could be used. Hence, noting that at zero field all fluctuations are close to zero (except at a critical point) and that the application of an external field provides in general an increase of the second central moment of the energy, we can further assume that at  $T_0$  the (field dependence of the) third central moment of the excess energy fluctuation  $M_3[\mathcal{U}']$  can be well approximated (in the field range of interest) by a first-order expansion in the second central moment  $M_2[\mathcal{U}']$ :

$$M_3[\mathcal{U}'](T_0, \mathfrak{F}_0) \cong \left( \frac{\partial M_3[\mathcal{U}']}{\partial M_2[\mathcal{U}']} \right)_{M_2[\mathcal{U}']=0} M_2[\mathcal{U}'](T_0, \mathfrak{F}_0), \quad (18)$$

where  $M_n[\mathcal{U}'] = \langle (\mathcal{U}' - \langle \mathcal{U}' \rangle)^n \rangle$  and we set  $M_3[\mathcal{U}']$  for  $M_2[\mathcal{U}'] = 0$  equal to zero, since a distribution with zero second central moment must have all central moments equal to zero. Using the previous equation in the definition of the gamma state parameter  $\delta_0$  (see, e.g., Ref. 1),

$$\delta_0(\mathfrak{F}_0) = \frac{M_3(\mathcal{U}')(T_0, \mathfrak{F}_0)}{2kT_0 M_2[\mathcal{U}'](T_0, \mathfrak{F}_0)}, \quad (19)$$

we readily see that

$$\frac{\partial \delta_0}{\partial \mathfrak{F}_0} \cong 0. \quad (20)$$

This means that  $\delta_0$ , which characterizes the asymmetry of the gamma distribution  $\rho(\mathcal{U}')$ , is independent of the field (a “stationary” condition).

Finally, as a very good approximation, the accessible phase-space fraction  $\epsilon$  can be considered independent of the field.

The use of these assumptions with the explicit expressions of the confined gamma state<sup>1</sup> means that at least for one geometry, defined by the geometry coefficient  $f_d$ , the ideal reduced or excess free energy change due to a change of the external applied field is

$$\Delta A'(T, \mathfrak{F}_0) = \Delta U'_0(\mathfrak{F}_0) - T_0 \Delta C'_{V0}(\mathfrak{F}_0) \Lambda(T), \quad (21)$$

with

$$\Lambda(T) = \frac{1}{\delta_0} + \frac{1}{\delta_0^2} \left( \frac{T}{T_0} \right) \ln[1 - \delta(T)], \quad (22)$$

$$\delta(T) = \frac{T_0 \delta_0}{T(1 - \delta_0) + T_0 \delta_0}, \quad (23)$$

and, obviously,

$$\Delta U'_0(\mathfrak{F}_0) = U'_0(\mathfrak{F}_0) - U'_0(0), \quad (24)$$

$$\Delta C'_{V0}(\mathfrak{F}_0) = C'_{V0}(\mathfrak{F}_0) - C'_{V0}(0). \quad (25)$$

$U'_0$  and  $C'_{V0}$  are the ideal reduced (or excess) internal energy and isochoric heat capacity at  $T_0$ , respectively.

Expressing at  $T_0$  the free energy change with a given QGE model for the field dependence (second assumption), we have

$$\Delta C'_{V0}(\mathfrak{F}_0) = \frac{\Delta U'_0(\mathfrak{F}_0) - \Delta A'_0(\mathfrak{F}_0)}{T_0 \Lambda_0}, \quad (26)$$

with

$$\Lambda_0 \equiv \Lambda(T_0) = \frac{1}{\delta_0} + \frac{1}{\delta_0^2} \ln(1 - \delta_0), \quad (27)$$

and where [cf. Eq. (14)]  $\Delta A'_0(\mathfrak{F}_0) = \Delta A_0(\mathfrak{F}_0) - \frac{1}{2} \mathcal{A} \mathfrak{F}_0^2$  is the excess free-energy change at  $T_0$  due to the field, with  $\Delta A_0(\mathfrak{F}_0)$  described by a given QGE model for the field dependence as derived in I. Hence

$$\begin{aligned} \Delta A'(T, \mathfrak{F}_0) &= \Delta A'_0(\mathfrak{F}_0) \left[ \frac{\Delta U'_0(\mathfrak{F}_0)}{\Delta A'_0(\mathfrak{F}_0)} \right. \\ &\quad \left. + \left( 1 - \frac{\Delta U'_0(\mathfrak{F}_0)}{\Delta A'_0(\mathfrak{F}_0)} \right) \frac{\Lambda(T)}{\Lambda_0} \right]. \end{aligned} \quad (28)$$

Equation (28) is completely defined if we have an expression for  $\Delta U'_0(\mathfrak{F}_0)/\Delta A'_0(\mathfrak{F}_0)$ . One of the simplest and most reasonable ways to express such a ratio is to expand  $\Delta U'_0(\mathfrak{F}_0)$  in a Taylor series in terms of  $\Delta A'_0(\mathfrak{F}_0)$ , using the fact that  $\Delta U'_0$  for  $\Delta A'_0 = 0$  is zero, and retaining again only the first-order term:

$$\Delta U'_0(\mathfrak{F}_0) \cong C_1 \Delta A'_0(\mathfrak{F}_0). \quad (29)$$

Hence we obtain

$$\Delta A'(T, \mathfrak{F}_0) = \Delta A'_0(\mathfrak{F}_0) \left[ C_1 + (1 - C_1) \frac{\Lambda(T)}{\Lambda_0} \right]. \quad (30)$$

We can eliminate  $C_1$  by considering the “infinite” temperature limit of  $M/\mathfrak{F}_0$  [cf. Eq. (1) of I], obtained by differentiating the total free-energy change [Eqs. (14) and (30)], yielding

$$\mathcal{A} = \frac{M'_0(\mathfrak{F}_0)}{\mathfrak{F}_0} \left[ C_1 + (1 - C_1) \frac{\Lambda_\infty}{\Lambda_0} \right] - \frac{V}{\zeta_0} \frac{\chi_\infty}{1 + f_d \chi_\infty}, \quad (31)$$

where  $\chi_\infty$  is the “infinite” temperature limit of the susceptibility and  $\Lambda_\infty = -1/(1 - \delta_0)$  is the infinite temperature limit of  $\Lambda(T)$ . In the last equation  $C_1 + (1 - C_1) \Lambda_\infty/\Lambda_0 = 0$  is the necessary and sufficient condition to match the results of Eq. (A4),

$$\mathcal{A} = - \frac{V}{\zeta_0} \frac{\chi_\infty}{1 + f_d \chi_\infty}, \quad (32)$$

leading to

$$C_1 = \frac{\Lambda_\infty}{\Lambda_\infty - \Lambda_0}. \quad (33)$$

At this point we have a completely analytical equation of state for the temperature and field dependence for a specific geometry of the system, defined as the reference geometry. Clearly, any model for  $\Delta A_0(\mathfrak{F}_0)$  as given in I [and hence via Eq. (14) for  $\Delta A'_0(\mathfrak{F}_0)$ ] yields a different equation of state. The explicit expressions at the reference geometry<sup>0</sup>  $f_d$  of free energy, electromagnetic moment, entropy and heat capacity (with a still unspecified field model) are

$$\begin{aligned} {}^0A'(T, \mathfrak{F}_0) &\equiv A'(T, \mathfrak{F}_0, {}^0f_d) \\ &= A'(T, 0) + \Delta {}^0A'(T, \mathfrak{F}_0) \\ &= A'(T, 0) + \Delta {}^0A'_0(\mathfrak{F}_0) \frac{\Lambda_\infty - \Lambda(T)}{\Lambda_\infty - \Lambda_0}, \end{aligned} \quad (34)$$

$$\begin{aligned} {}^0M(T, \mathfrak{F}_0) &\equiv M(T, \mathfrak{F}_0, {}^0f_d) \\ &= {}^0M'_0(\mathfrak{F}_0) \frac{\Lambda_\infty - \Lambda(T)}{\Lambda_\infty - \Lambda_0} \\ &\quad + \frac{V}{\zeta_0} \frac{\chi_\infty}{1 + {}^0f_d \chi_\infty} \mathfrak{F}_0, \end{aligned} \quad (35)$$

$$\begin{aligned} {}^0S'(T, \mathfrak{F}_0) &\equiv S'(T, \mathfrak{F}_0, {}^0f_d) \\ &= S'(T, 0) + \Delta {}^0S'(T, \mathfrak{F}_0) \\ &= S'(T, 0) \\ &\quad + \frac{\Delta {}^0A'_0(\mathfrak{F}_0)}{T_0} \frac{1}{\Lambda_\infty - \Lambda_0} \{ \delta(T) + \ln[1 - \delta(T)] \}, \end{aligned} \quad (36)$$

$$\begin{aligned} {}^0C'_V(T, \mathfrak{F}_0) &\equiv C'_V(T, \mathfrak{F}_0, {}^0f_d) \\ &= C'_V(T, 0) + \Delta {}^0C'_V(T, \mathfrak{F}_0) \\ &= C'_V(T, 0) + \frac{\Delta {}^0A'_0(\mathfrak{F}_0)}{T_0} \frac{1}{\Lambda_\infty - \Lambda_0} \left( \frac{\delta(T)}{\delta_0} \right)^2, \end{aligned} \quad (37)$$

where, obviously,  ${}^0M'_0(\mathfrak{F}_0) = -\partial \Delta {}^0A'_0(\mathfrak{F}_0)/\partial \mathfrak{F}_0$ .

For fluid dielectric systems  $\chi_\infty \cong n_{\text{opt}}^2 - 1$ , with  $n_{\text{opt}}$  typically the optical refractive index, since this corresponds to the situation where the contribution to  $\chi$  from molecular rotations, librations, and vibrations is zero.<sup>17,18</sup> In practice,  $n_{\text{opt}}$  only weakly depends on temperature and frequency in the optical range and hence can be used to evaluate  $\mathcal{A}$ . For magnetic systems,  $\mathcal{A}$  reflects the effect of both diamagnetism and Van Vleck (or temperature-independent) paramagnetism,<sup>6</sup> and  $\chi_\infty$  is approximately given by the Pascal constants.<sup>19</sup>

The expressions above can be generalized to a system with a geometry coefficient  $f_d$  different from the reference geometry  ${}^0f_d$  using Eq. (4) of I:

$$M(T, \mathfrak{F}_0, f_d) = \frac{{}^0M(T, \mathfrak{F}_0)}{1 + (f_d - {}^0f_d)\zeta_0 {}^0M(T, \mathfrak{F}_0)/(V\mathfrak{F}_0)}, \quad (38)$$

and hence

$$A'(T, \mathfrak{F}_0, f_d) = A'(T, 0) - \int_0^{\mathfrak{F}_0} M(T, \mathfrak{F}'_0, f_d) d\mathfrak{F}'_0 - \frac{1}{2} \mathcal{A} \mathfrak{F}_0^2. \quad (39)$$

Note that at zero field the free energy and any thermodynamic property that is not obtained by derivatives of free energy in the field are independent of the shape factor and hence, as indicated,  $A'(T, 0)$  is not a function of  $f_d$ . From Eq. (39) the whole ideal reduced thermodynamics follows, e.g.,

$$S'(T, \mathfrak{F}_0, f_d) = S'(T, 0) + \int_0^{\mathfrak{F}_0} \left( \frac{\partial M(T, \mathfrak{F}'_0, f_d)}{\partial T} \right) d\mathfrak{F}'_0, \quad (40)$$

$$C'_V(T, \mathfrak{F}_0, f_d) = C'_V(T, 0) + T \int_0^{\mathfrak{F}_0} \left( \frac{\partial^2 M(T, \mathfrak{F}'_0, f_d)}{\partial T^2} \right) d\mathfrak{F}'_0, \quad (41)$$

etc., and so a complete theoretical equation of state in temperature, field, and geometrical shape is obtained. However, for shape-independent properties such as  $\chi$ , the EOS needs only to be evaluated at the reference geometry  ${}^0f_d$ . Note that this whole derivation can be readily generalized to ellipsoidal systems where the external field is not aligned along one of the ellipsoidal axes.<sup>20</sup>

## C. Special conditions

### 1. Weak-field limit: Gamma [ $\mathcal{U}'$ ] + Gaussian [ $\mathcal{M}'$ ] EOS

First we will investigate the weak-field limit of the general EOS, Eq. (34). From Eq. (A1) we have at  $T_0$

$$\frac{\partial {}^0M'_0(\mathfrak{F}_0)}{\partial \mathfrak{F}_0} = \frac{\partial {}^0M(T_0, \mathfrak{F}_0)}{\partial \mathfrak{F}_0} + \mathcal{A} = \beta_0 {}^0K_0, \quad (42)$$

where  ${}^0K_0 = \langle (\mathcal{M}' - \langle \mathcal{M}' \rangle)^2 \rangle$  with the ensemble average taken at  $T_0$  and  $f_d = {}^0f_d$ . Hence in the limit of weak field we can express  ${}^0M'_0$  using a Taylor expansion in the field up to the first order,

$${}^0M'_0(\mathfrak{F}_0) \cong \beta_0 {}^0K_0 \mathfrak{F}_0, \quad (43)$$

with  ${}^0K_0 = {}^0\kappa_0[\mathcal{M}']$  the second central moment of  $\mathcal{M}'$  evaluated at  $T_0$ ,  $f_d = {}^0f_d$ , and  $\mathfrak{F}_0 = 0$ . So from Eq. (35) we have

$${}^0M(T, \mathfrak{F}_0) = \beta_0 {}^0K_0 \mathfrak{F}_0 \frac{\Lambda_\infty - \Lambda(T)}{\Lambda_\infty - \Lambda_0} + \frac{V}{\zeta_0} \frac{\chi_\infty}{1 + {}^0f_d \chi_\infty} \mathfrak{F}_0, \quad (44)$$

which is exactly the expression obtained when  $\Delta^0 A'_0(\mathfrak{F}_0)$  is modeled by a Gaussian distribution for the fluctuations of  $\mathcal{M}'$  [see Eq. (27) of I]: a gamma [ $\mathcal{U}'$ ] + Gaussian [ $\mathcal{M}'$ ] EOS. This clearly means that any model of  $\Delta^0 A'_0(\mathfrak{F}_0)$  tends to the Gaussian one in the limit of weak field, and so Eq. (44) is always valid in the weak-field limit, regardless of the specific field model used for the general EOS.

Moreover, in this limit we can express  $\beta_0 {}^0K_0$  in terms of  $\chi^0_0$  (i.e.,  $\chi$  at  $T_0$ ,  $\mathfrak{F}_0 = 0$ ) and  $\chi_\infty$  via Eq. (A5),

$$\beta_0 {}^0K_0 = \frac{V}{\zeta_0} \frac{\chi^0_0 - \chi_\infty}{(1 + {}^0f_d \chi^0_0)(1 + {}^0f_d \chi_\infty)}, \quad (45)$$

so that the weak-field EOS is completely defined in terms of the parameters  $\delta_0$ ,  $\chi^0_0$ ,  $\chi_\infty$ , and  ${}^0f_d$  at  $T_0$ . Specifically, combining Eq. (2) of I and Eqs. (44) and (45) we obtain for the weak-field susceptibility

$$\chi^0(T) = \frac{(\chi^0_0 - \chi_\infty)z(T) + \chi_\infty(1 + {}^0f_d \chi^0_0)}{1 - {}^0f_d[(\chi^0_0 - \chi_\infty)z(T) - \chi^0_0]}, \quad (46)$$

with  $z(T) = [\Lambda_\infty - \Lambda(T)]/(\Lambda_\infty - \Lambda_0)$ .

### 2. Curie's law: Gaussian [ $\mathcal{U}'$ ] + Gaussian [ $\mathcal{M}'$ ] EOS

The well-known Curie's law,  $\chi^0(T) = C/T + a$  with  $C$  the Curie constant, reflects the fact that for many systems the weak-field susceptibility is basically inversely proportional to the temperature. Usually, Curie's law is derived for paramagnetic systems, where the effect of shape is unimportant, so that [cf. Eq. (3) of I]  $\chi^0 \cong \zeta_0 {}^0M^0/(V\mathfrak{F}_0)$ . Using Eqs. (44) and (45) with the explicit expressions of  $\Lambda(T)$ ,  $\Lambda_0$ , and  $\Lambda_\infty$  we thus obtain

$$\chi^0(T) \cong (\chi^0_0 - \chi_\infty) \frac{T(1 - \delta_0) \ln\{1 - \delta(T)\} + T_0 \delta_0}{T(1 - \delta_0) \ln\{1 - \delta_0\} + T_0 \delta_0} + \chi_\infty. \quad (47)$$

This expression has a  $1/T$  dependence only in the limit  $\delta_0 \rightarrow 0$ , which corresponds to a Gaussian state<sup>1</sup> for the energy fluctuations  $\mathcal{U}'$ . In that limit we have

$$\chi^0(T) \cong (\chi^0_0 - \chi_\infty) \frac{T_0}{T} + \chi_\infty, \quad (48)$$

which is Curie's law. The interesting point is that usually this law is derived for a set of ideal noninteracting classical or quantum spins, where in the absence of an external field the energy distribution  $\rho(\mathcal{U}')$  is a Dirac  $\delta$  function. Since a  $\delta$  function is just a Gaussian with variance tending to zero, it is not surprising that to obtain Curie's law from the distribution point of view, one has to couple a Gaussian [ $\mathcal{U}'$ ] state (see, e.g., Ref. 1) to a Gaussian [ $\mathcal{M}'$ ] state, yielding a Gaussian [ $\mathcal{U}'$ ] + Gaussian [ $\mathcal{M}'$ ] EOS.<sup>21</sup>

### 3. Gamma [ $\mathcal{U}'$ ] + discrete uniform [ $\mathcal{M}'$ ] EOS

In Sec. III we illustrate the behavior of a complete equation of state modeling  $\Delta^0 A'_0(\mathfrak{F}_0)$  beyond the Gaussian approximation. As a field model we use the discrete uniform statistical state,<sup>6</sup> modeling the distribution of  $\mathcal{M}'$  as the convolution of discrete uniform ones. For this statistical state we have

$$\Delta^0 A'_0(\mathfrak{F}_0) = \frac{M'_s}{(n/2)\beta_0\Delta m'} \ln \left\{ \frac{(n+1) \sinh\{\frac{1}{2}\beta_0\Delta m'\mathfrak{F}_0\}}{\sinh\{[(n+1)/2]\beta_0\Delta m'\mathfrak{F}_0\}} \right\}, \quad (49)$$

$${}^0M'_0(\mathfrak{F}_0) = M'_s B_{n/2} \left( \frac{n}{2} \beta_0 \Delta m' \mathfrak{F}_0 \right), \quad (50)$$

where  $n$ ,  $\Delta m'$ , and  $M'_s$  are parameters related to physical properties of the system and  $B_J(x)$  is the Brillouin function.<sup>6</sup> Inserting this into the general equations (34)–(37), we obtain, e.g., for the electromagnetic moment:

$${}^0M(T, \mathfrak{F}_0) = M'_s B_{n/2} \left( \frac{n}{2} \beta_0 \Delta m' \mathfrak{F}_0 \right) \frac{\Lambda_\infty - \Lambda(T)}{\Lambda_\infty - \Lambda_0} + \frac{V}{\zeta_0} \frac{\chi_\infty}{1 + {}^0f_d \chi_\infty} \mathfrak{F}_0. \quad (51)$$

This specific EOS will be referred to as the  $\Gamma$  [ $\mathcal{U}'$ ] + discrete uniform [ $\mathcal{M}'$ ] EOS.

## III. RESULTS AND DISCUSSION

In this section we will first test the general weak-field limit of the EOS on the thermal behavior of the weak-field dielectric constant of water at different isochores (densities), ranging from gas to liquid. Second, we will analyze at two specific isochores ( $\rho_N = 45.0$  and  $55.51$  mol/dm<sup>3</sup>) the field dependence of the dielectric constant of water at  $T_0 = 550$  and  $300$  K, respectively, using both experimental data and simulations of the SPC/E water model.<sup>22</sup> Third, at the same two isochores the behavior of the  $\Gamma$  [ $\mathcal{U}'$ ] + discrete uniform [ $\mathcal{M}'$ ] EOS will be investigated.

### A. Weak-field temperature dependence of $\epsilon_r$

First, we analyzed the thermal behavior of the weak-field dielectric constant  $\epsilon_r(T, 0)$  of water at different isochores. In this weak-field limit all possible EOS converge towards the gamma [ $\mathcal{U}'$ ] + Gaussian [ $\mathcal{M}'$ ] EOS, where  $\epsilon_r(T, 0) = 1 + \chi^0(T)$  with  $\chi^0(T)$  given by Eq. (46).

We investigated a range of densities, varying from  $0.5$  to  $55$  mol/dm<sup>3</sup>. At each density we used experimental  $\epsilon_r(T, 0)$  data from the temperature–density regression of Fernandez *et al.*<sup>23</sup> and Wagner and Kruse,<sup>24</sup> which is based on a compiled experimental database.<sup>25</sup> For all isochores the temperature ranges from the coexistence line up to  $873$  K, except for the two highest densities ( $773$  K for  $50$  mol/dm<sup>3</sup>;  $603$  K for  $55$  mol/dm<sup>3</sup>). Error bars in  $\epsilon_r(T, 0)$  were taken from Figs. 6–10 and Table 9 of Ref. 23. Note that especially at low density (and high temperature) the uncertainties are relatively large, due to the lack of sufficient experimental data. At each density we set  $T_0$  about  $20$  K above the coexistence

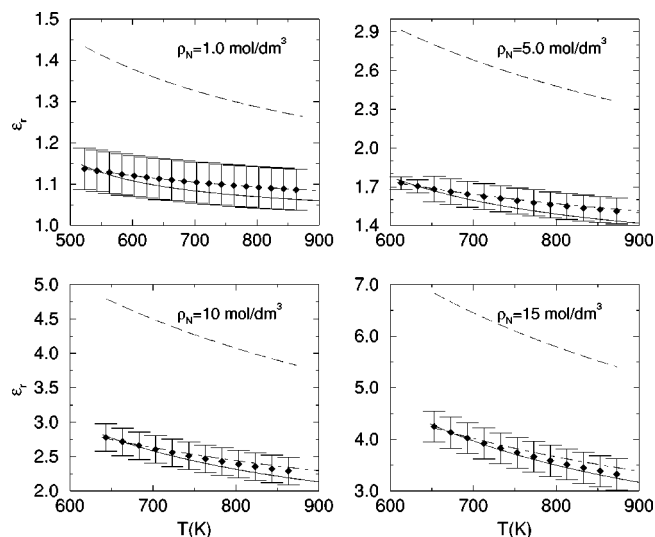


FIG. 1. Weak-field dielectric constant  $\epsilon_r(T, 0)$  of water as a function of temperature; experimental data ( $\blacklozenge$ ) with uncertainties, gamma [ $\mathcal{U}'$ ] + Gaussian [ $\mathcal{M}'$ ] EOS [Eq. (46), —], Curie's law [Eq. (48), ---], and the Booth equation [Eq. (53), ···].

line, and the corresponding gamma state parameter  $\delta_0$  was obtained from the previously developed QGE water equation of state,<sup>4,26</sup> based on an analysis of  $A'(T, 0)$  vs  $T$  along isochores. The optical refractive index  $n_{\text{opt}}$  was taken at  $T_0$  and  $\lambda = 589$  nm from the temperature–density–wavelength correlation of Wagner and Kruse<sup>24</sup> and Schiebener *et al.*<sup>27,28</sup> Using these data, at each density the gamma [ $\mathcal{U}'$ ] + Gaussian [ $\mathcal{M}'$ ] EOS expression of  $\epsilon_r(T, 0)$  was fitted with a nonlinear least-square procedure to the experimental data, yielding the optimal value of the reference geometry factor  ${}^0f_d$ . Note that instead of a least-square fit, we could also obtain the value of  ${}^0f_d$  at each isochore from just one value of  $\epsilon_r$  at a temperature different from  $T_0$ .

Results for  $\epsilon_r$  are given in Figs. 1–3. At all densities the gamma [ $\mathcal{U}'$ ] + Gaussian [ $\mathcal{M}'$ ] EOS provides an accurate description of the thermal behavior of the weak-field dielectric constant of water, indicating that at every isochore there is at least one reference geometry  ${}^0f_d$  where the assumptions of the EOS are valid. In Fig. 4 these optimal values of  ${}^0f_d$  are given as a function of density. Also indicated is the “allowed” range of  ${}^0f_d$  values, which provide still an acceptable description of  $\epsilon_r(T, 0)$ , i.e., within the experimental error bars, roughly corresponding to a 90% confidence interval of the statistical  $\chi^2$  test. In general the values of  ${}^0f_d$  are small ( $\leq 0.03$ ). This corresponds to very elongated ellipsoidal samples with very small depolarizing field<sup>6</sup>  $-{}^0f_d {}^0M_e/V\epsilon_0$ , meaning that the system is not very much “perturbed” by the external field, and might react in a rather “simple” way to field. This is in agreement with one of the assumptions, the “stationary” condition [Eq. (20)], which assumes that both the second and the third central energy moments react in a similar way to the field. As can also be seen from Fig. 4, at very low density (with virtually no correlation within the system) the model provides the same accuracy for every sample shape. However, with increasing density the allowed range of  ${}^0f_d$  values becomes more narrow, until at  $55.51$

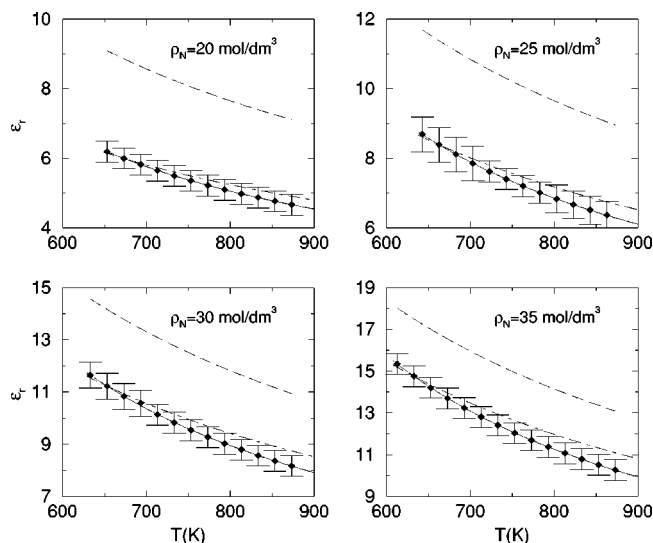


FIG. 2. Weak-field dielectric constant  $\epsilon_r(T,0)$  of water as a function of temperature; experimental data ( $\blacklozenge$ ) with uncertainties, gamma [ $\mathcal{U}'$ ] + Gaussian [ $\mathcal{M}'$ ] EOS [Eq. (46), —], Curie's law [Eq. (48), ----], and the Booth equation [Eq. (53), ---].

mol/dm<sup>3</sup> (=1.0 g/cm<sup>3</sup>) a specific value of  $^0f_d=0.015$  has been reached.

For comparison, also two other models are presented in Figs. 1–3, first, the Curie's law expression of  $\chi^0(T)$ , Eq. (48), based on a Gaussian [ $\mathcal{U}'$ ] + Gaussian [ $\mathcal{M}'$ ] EOS. It is clear that this model is less accurate than the gamma [ $\mathcal{U}'$ ] + Gaussian [ $\mathcal{M}'$ ] expression, Eq. (46), except for lower densities ( $\rho_N \lesssim 15$  mol/dm<sup>3</sup>), where both models are comparable. Deviations are more pronounced at high density. Second, in the 1950s, Booth<sup>29–31</sup> extended the Onsager theory to water at high field strengths and obtained

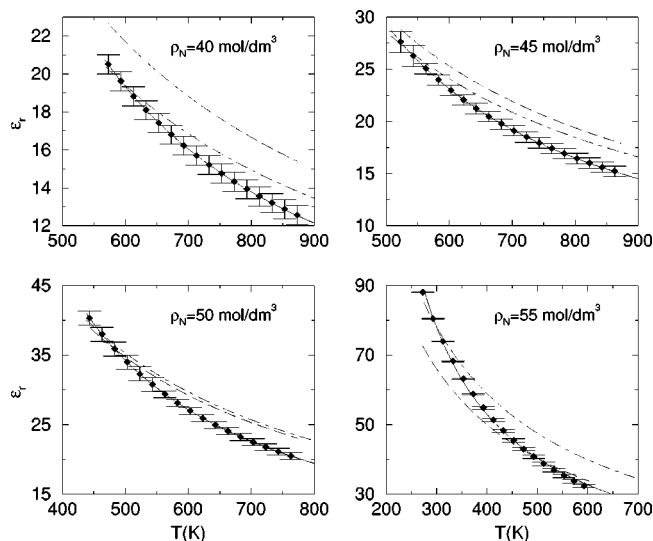


FIG. 3. Weak-field dielectric constant  $\epsilon_r(T,0)$  of water as a function of temperature; experimental data ( $\blacklozenge$ ) with uncertainties, gamma [ $\mathcal{U}'$ ] + Gaussian [ $\mathcal{M}'$ ] EOS [Eq. (46), —], Curie's law [Eq. (48), ----], and the Booth equation [Eq. (53), ---].

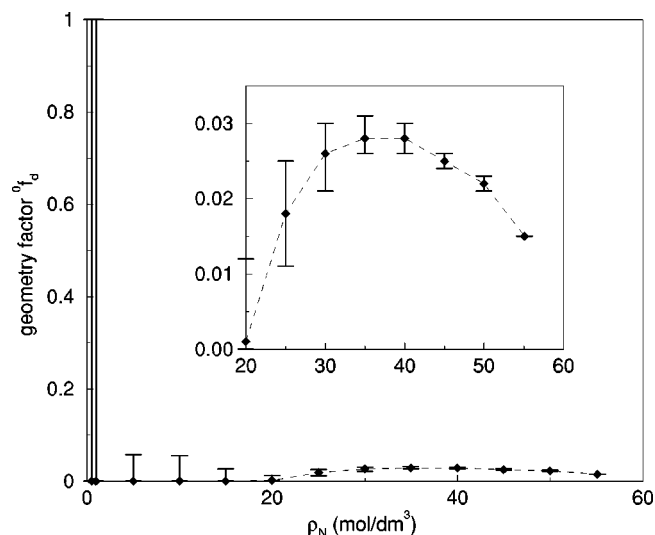


FIG. 4. Optimal values of the geometry factor  $^0f_d$  for water as a function of density; optimal value ( $\blacklozenge$ ) with acceptable variations (error bars) for the gamma [ $\mathcal{U}'$ ] + Gaussian [ $\mathcal{M}'$ ] EOS.

$$\epsilon_r(T, E) = n_{\text{opt}}^2 + \frac{7\rho_N\mu(n_{\text{opt}}^2 + 2)}{3\epsilon_0\sqrt{73}E} \mathcal{L}\left(\frac{\sqrt{73}\mu(n_{\text{opt}}^2 + 2)E}{6kT}\right), \quad (52)$$

with  $\mathcal{L}(x) = \coth(x) - 1/x$  the Langevin function and  $\mu = 1.85$  D the dipole moment of an ideal-gas water molecule. The weak-field limit is

$$\epsilon_r(T, 0) = n_{\text{opt}}^2 + \frac{7\rho_N\mu^2(n_{\text{opt}}^2 + 2)^2}{54\epsilon_0kT}. \quad (53)$$

From the figures it is clear that the Booth equation [Eq. (53)] only gives reasonable results at the two highest densities, although not as accurate as Eq. (46), at all other densities its predictions of the weak-field dielectric constant are significantly larger than experimental values.

## B. Field dependence of $\epsilon_r$

Second, we analyzed the field dependence of the polarization of water at two specific liquid isochores at the corresponding optimal reference geometry  $^0f_d$  as obtained above:  $\rho_N = 45.0$  mol/dm<sup>3</sup>,  $T_0 = 550$  K,  $^0f_d = 0.025$  and  $\rho_N = 55.51$  mol/dm<sup>3</sup>,  $T_0 = 300$  K,  $^0f_d = 0.015$ . Using the experimental values of  $n_{\text{opt}}$  and hence a nonzero value of  $\mathcal{A}$  [see Eq. (32)], we assessed the optimal QGE field models that can be combined further on with the gamma state temperature model.

To observe clear saturation of the polarization one has to reach fields of the order of  $10^{10}$  V/m (= 1 V/Å); however, in practice only fields up to  $\sim 10^{-3}$  V/Å can be reached due to experimental difficulties because of the relatively large conductivity of water,<sup>32</sup> promoting currents through the sample at high field strength. At fields of  $\sim 10^{-3}$  V/Å, however, one can observe the first deviations from the linear (Gaussian) response, the so-called nonlinear dielectric effect (NDE):<sup>33,34</sup>

$$\epsilon_r(E) \approx \epsilon_r(0) + \beta_{\text{NDE}}E^2, \quad (54)$$

with  $\beta_{\text{NDE}} = -1080 \times 10^{-18}$  m<sup>2</sup>/V<sup>2</sup> the NDE coefficient of water<sup>34</sup> at 55 mol/dm<sup>3</sup> and 300 K. No values of  $\beta_{\text{NDE}}$  are

TABLE I. Dielectric constant  $\epsilon_r$  of SPC/E water as a function of electric field  $E$  at two different densities, obtained by molecular dynamics simulations.

$E$ (V/Å)	$\rho_N = 45.0$ mol/dm <sup>3</sup>		$\rho_N = 55.51$ mol/dm <sup>3</sup>	
	$T = 550$ K		$T = 300$ K	
	$\epsilon_r(E)$	$t_{\text{sim}}$ (ps)	$\epsilon_r(E)$	$t_{\text{sim}}$ (ps)
0	25.43 ± 0.63	600	70.18 ± 2.24	5000
0.004	25.65 ± 1.38	300	71.89 ± 4.95	1200
0.008	24.28 ± 0.61	300	68.74 ± 2.40	1200
0.0167	25.25 ± 0.42	300	60.96 ± 0.58	300
0.03	23.76 ± 0.15	300	52.38 ± 0.28	300
0.0525	20.81 ± 0.08	300	38.36 ± 0.11	300
0.085	17.10 ± 0.03	300	27.25 ± 0.04	300
0.122	14.01 ± 0.01	300	20.66 ± 0.03	300
0.186	10.600 ± 0.005	300	14.67 ± 0.01	300
0.325	7.099 ± 0.002	300	9.272 ± 0.004	300
0.5	5.188 ± 0.001	300	6.543 ± 0.002	300

available at other conditions. Therefore, additional data at higher field strength and/or other densities may come from molecular simulations.

Recently, Yeh and Berkowitz<sup>35</sup> calculated  $\epsilon_r(E)$  at 300 K from molecular dynamics simulation using the extended simple point charge (SPC/E) water model<sup>22</sup> with Ewald summation. This model reproduces in the best way, among the different (nonpolarizable) water models, various static and dynamic properties of water.<sup>36,37</sup> Yeh and Berkowitz observed that  $\epsilon_r(E)$  of SPC/E agrees rather well with the Booth equation [Eq. (52)], suggesting that SPC/E might be used as a reasonable model for real water. To obtain values of  $\epsilon_r(T_0, E)$  for water at both densities, we performed molecular dynamics simulations of the SPC/E model with an external electric field using particle mesh Ewald<sup>38,39</sup> (PME) with conducting boundary conditions for the long-range electrostatic interactions. For nonzero field  $E$ , the dielectric constant was determined from the average polarization of the system;<sup>35</sup> the zero-field values were determined from the variance of the total dipole moment of the system,  $\kappa_2[\mathcal{M}']$ , using the appropriate Ewald fluctuation formula<sup>40,41</sup>  $\epsilon_r = 1 + \kappa_2[\mathcal{M}']/(3\epsilon_0 kTV)$ . Simulations were performed using the GROMACS 3.0 software package,<sup>42–44</sup> with periodic boundary conditions and a leapfrog Verlet algorithm using a time step  $\Delta t = 1$  fs (45 mol/dm<sup>3</sup>) and 2 fs (55.51 mol/dm<sup>3</sup>), respectively. The temperature was kept constant (at 550 and 300 K, respectively) by a Berendsen thermostat<sup>45</sup> with cou-

pling time  $\tau_T = \Delta t$  mimicking a Gaussian thermostat.<sup>46,47</sup> Constraints were handled by SETTLE.<sup>48</sup> Each state point was equilibrated for 50 ps, and the total length of the production runs ( $t_{\text{sim}}$ ) is given in Table I, as well as the values of  $\epsilon_r(E)$ . Error bars were determined by the block-average method.<sup>49–51</sup>

The values in Table I at 55 mol/dm<sup>3</sup> agree perfectly with the values of Yeh and Berkowitz, and the zero-field limit is in agreement with the value of Svishchev and Kusalik<sup>52</sup> (69.6 ± 1.5). At 45 mol/dm<sup>3</sup> the SPC/E value of  $\epsilon_r(T_0, 0)$  matches the experimental value very well (25.83); at 55 mol/dm<sup>3</sup> it is lower than experiment (78.03). To have reasonable high-field data for water, we scaled  $\epsilon_{r,\text{SPC/E}}(T_0, E) - n_{\text{opt}}^2$  at both densities to match the experimental zero-field limit: for the two densities the scaling factor  $c = [\epsilon_{r,\text{exp}}(T_0, 0) - n_{\text{opt}}^2]/[\epsilon_{r,\text{SPC/E}}(T_0, 0) - n_{\text{opt}}^2]$  was 1.01 and 1.11, respectively.

For both densities, we calculated at the optimal geometry  ${}^0f_d$  the values of  $M/(V\epsilon_0) = P/\epsilon_0$  versus  $E_0$  based on the (scaled) SPC/E data. For the analysis of the polarization we excluded the NDE data, since they are measured at relatively weak field and hence do not affect the analysis. For the parametrization of the various QGE field models as derived in I we used the values of the initial slope,

$$\frac{\partial^0 M_0^0/(V\epsilon_0)}{\partial E_0} = \frac{\partial^0 P_0^0/\epsilon_0}{\partial E_0} = \frac{\epsilon_r(T_0, 0) - 1}{1 + {}^0f_d[\epsilon_r(T_0, 0) - 1]}$$

TABLE II. Root-mean-square deviations (RMSD) normalized by  $M'_s$  of different statistical states (QGE field models) from the (scaled) SPC/E data. Equation numbers refer to the expressions given in Ref. 6.

Statistical state	$\rho_N = 45.0$ mol/dm <sup>3</sup>	$\rho_N = 55.51$ mol/dm <sup>3</sup>
	RMSD/ $M'_s$	RMSD/ $M'_s$
Gaussian (Eq. I-27)	1.279	2.284
Continuous uniform (Eq. I-37)	0.061	0.061
Beta (Eq. I-34)	0.007 ( $a = 0.06$ )	0.008 ( $a = 0.08$ )
Binomial (Eq. I-46)	0.013	0.018
Symmetrized binomial (Eq. I-49)	0.013 ( $p = 0.50$ )	0.018 ( $p = 0.50$ )
Double binomial (Eq. I-52)	0.006 ( $p = 0.451$ )	0.014 ( $p = 0.449$ )
Discrete uniform (Eq. I-41)	0.004 ( $n = 2$ )	0.010 ( $n = 3$ )
$N_{\text{data}}$	11	11
$f_d$	0.025	0.015

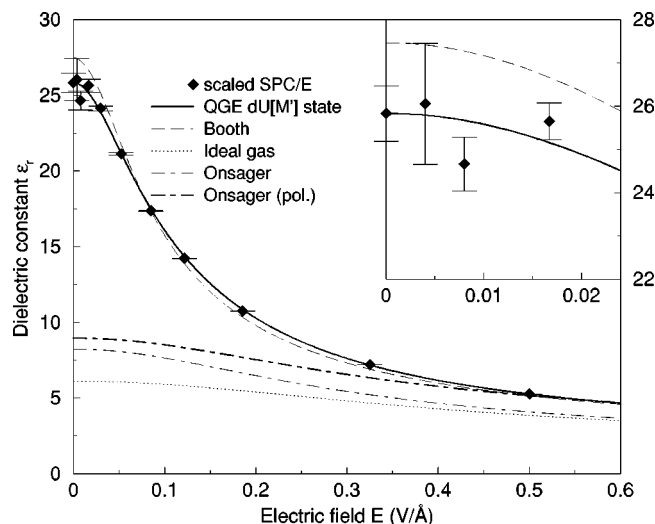


FIG. 5. Dielectric constant  $\epsilon_r$  of water at  $\rho_N = 45.0$  mol/dm<sup>3</sup>,  $T_0 = 550$  K as a function of electric field  $E$ : scaled SPC/E data, the QGE discrete uniform (dU) state [Eq. (50)], the Booth equation [Eq. (52)], the “ideal gas” [Eq. (58) of I], nonpolarizable Onsager [Eq. (59) of I], and polarizable Onsager models [Eq. (55)].

and  $M'_s/(V\epsilon_0) = P'_s/\epsilon_0 = 1.80$  and  $2.70$  V/Å for  $\rho_N = 45$  and  $55$  mol/dm<sup>3</sup>, respectively. For some models (beta, symmetrized binomial, double binomial, and discrete uniform) we used a nonlinear fit to obtain the third parameter (see I).

For all field models (statistical states) the root mean square deviations (RMSD's) from the scaled SPC/E data, divided by the maximum reduced em moment  $M'_s$ , are given in Table II. For both densities the two most accurate models are the beta state and the discrete uniform state with  $\text{RMSD}/M'_s \leq 1\%$ . As expected, the Gaussian model is only valid for weak fields ( $E_0 \leq 0.03$  V/Å). Two other models with a small RMSD value are the binomial (=symmetrized

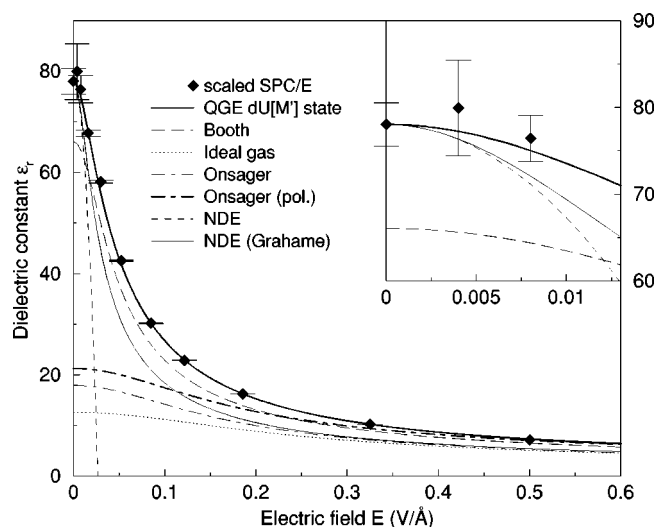


FIG. 6. Dielectric constant  $\epsilon_r$  of water at  $\rho_N = 55.51$  mol/dm<sup>3</sup>,  $T_0 = 300$  K as a function of electric field  $E$ : scaled SPC/E data, the QGE discrete uniform (dU) state [Eq. (50)], the Booth equation [Eq. (52)], the “ideal gas” [Eq. (58) of I], nonpolarizable Onsager [Eq. (59) of I], and polarizable Onsager models [Eq. (55)]. Also included are the NDE expression [Eq. (54)] and Grahame's empirical function [Eq. (56)].

binomial with  $p=0.5$ ) and double binomial states with  $\text{RMSD}/M'_s < 2\%$ .

In Figs. 5 and 6 we present for both densities  $\epsilon_r(T_0, E)$  as a function of  $E$ , independent of shape (i.e.,  $f_d$ ). Clearly, the discrete uniform model, Eq. (50), gives for both isochores a very accurate description of the “experimental” (i.e., scaled SPC/E) data. The same is true for the beta model, Eq. (34) of I (not shown). The Booth equation [Eq. (52)] gives a reasonable description, especially at  $45$  mol/dm<sup>3</sup>, although the weak-field limit is not correct. For comparison, we also included the “ideal-gas” model [Eq. (58) of I], the nonpolarizable Onsager [Eq. (59) of I], and polarizable Onsager model,<sup>53</sup>

$$\epsilon_r - 1 = \frac{\rho_N \mu}{\epsilon_0 E} \frac{(2\epsilon_r + 1)(n_{\text{opt}}^2 + 2)}{2\epsilon_r + n_{\text{opt}}^2} \mathcal{L} \left( \beta \mu E \frac{\epsilon_r(n_{\text{opt}}^2 + 2)}{2\epsilon_r + n_{\text{opt}}^2} \right) + \frac{3\epsilon_r(n_{\text{opt}}^2 - 1)}{2\epsilon_r + n_{\text{opt}}^2}, \quad (55)$$

using  $\mu = 1.85$  D as the experimental ideal-gas dipole moment. All three models fail to describe the experimental data, including the weak-field limit. At  $55$  mol/dm<sup>3</sup> (Fig. 6), we also include the NDE expression [Eq. (54)], which fails above  $E \approx 10^{-3}$  V/Å. Marcus and Hefter<sup>34</sup> and Grahame<sup>54</sup> have proposed an empirical formula for the differential dielectric constant,  $\epsilon_d(E) \equiv \partial(P/\epsilon_0)/\partial E$ , based on similarity

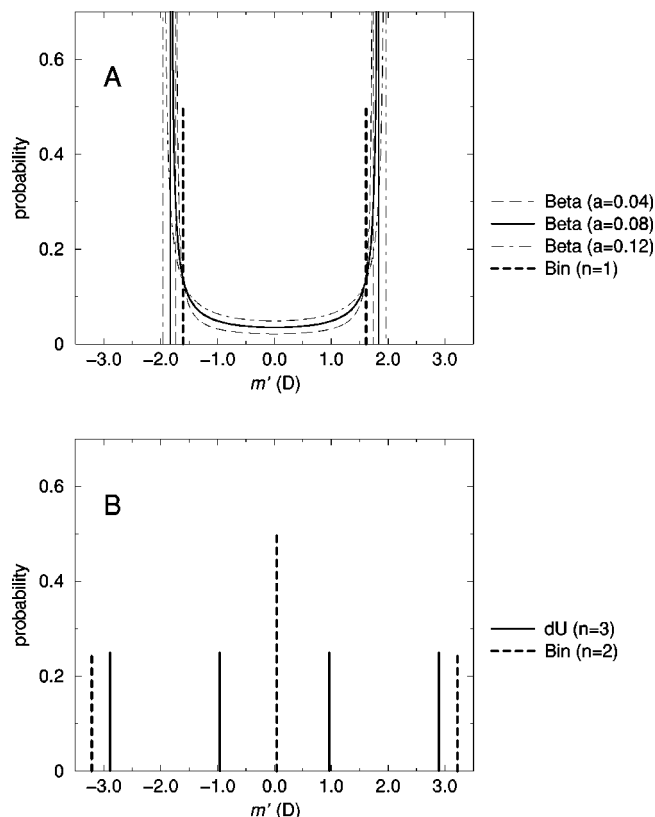


FIG. 7. Basic polarization distributions of water at  $55.51$  mol/dm<sup>3</sup> for various states: (A) Beta and binomial states with  $\sim 0.85$  water molecules per basic distribution; see Table III. (B) Discrete uniform and binomial states with  $\sim 1.35$  water molecules per basic distribution.

TABLE III. Allowed range of parameter values for the beta and discrete uniform statistical states with  $\text{RMSD}/M'_s \leq 1\%$ . Optimal parameter values are indicated with an asterisk.  $N/\mathbb{N}$  is the number of water molecules corresponding to a basic distribution. For comparison also the binomial state is presented. Note that since the binomial distribution is closed under convolution, the parameter  $n$  is in that case redundant.

Statistical state	$\rho_N = 45.0 \text{ mol/dm}^3$			$\rho_N = 55.51 \text{ mol/dm}^3$		
	Parameter	$\text{RMSD}/M'_s$	$N/\mathbb{N}$	Parameter	$\text{RMSD}/M'_s$	$N/\mathbb{N}$
Beta	$a = 0.02$	0.010	1.10	$a = 0.04$	0.010	0.81
	$a = 0.06^*$	0.007	1.18	$a = 0.08^*$	0.006	0.87
	$a = 0.10$	0.010	1.27	$a = 0.12$	0.010	0.93
Discrete uniform	$n = 2^*$	0.004	1.58			
	$n = 3$	0.006	1.90	$n = 3^*$	0.010	1.35
Binomial	$n = 1^*$	0.013	1.06	$n = 1^*$	0.018	0.75
	$n = 2^*$	0.013	2.11	$n = 2^*$	0.018	1.50

with the Booth equation:  $\epsilon_d(E) = n_{\text{opt}}^2 + [\epsilon_r(0) - n_{\text{opt}}^2]/(1 + bE^2)$ . Upon integrating this expression, we obtain for the (integral) dielectric constant  $\epsilon_r(E) \equiv (P/\epsilon_0)/E$  that is used in I and this paper:

$$\epsilon_r(E) = n_{\text{opt}}^2 + \frac{\epsilon_r(0) - n_{\text{opt}}^2}{\sqrt{b}E} \arctan(\sqrt{b}E). \quad (56)$$

Expanding this expression in  $E$  and comparing with Eq. (54), we see that  $b = -3\beta_{\text{NDE}}/[\epsilon_r(0) - n_{\text{opt}}^2]$ . Although the trend of Eq. (56) is correct, there are rather large discrepancies with the “experimental” data and the Booth equation.

Interestingly, at both densities the optimal beta distributions with parameter values  $a = 0.06$  and  $0.08$  are continuous but strongly peaked at the two end points of their domain (“U shaped”); see Fig. 7(A). Hence the two optimal field models (beta and discrete uniform) suggest that the distribution of the electric moment is discretelike and defined by the convolution of “simple” independent distributions (basic distributions) with only a few possible values. However, the “experimental” polarization curves do not allow one to evaluate the exact number of such discretelike polarization states. The same holds, for example, when one wants to obtain the frequency spectrum of a solid by “inversion” of the heat-capacity curve.<sup>3</sup> To investigate this point, we varied the parameter  $a$  or  $n$  of the beta and discrete uniform models, respectively, in such a way that the  $\text{RMSD}/M'_s$  value remained below 1%. Results are given in Table III, and the corresponding basic distributions for  $\rho_N = 55.51 \text{ mol/dm}^3$  are shown in Fig. 7. Note that ratio between the number of water molecules  $N$  and the total number of basic distributions  $\mathbb{N}$  is not identical for the various models and parameter values, but is always about 1 at both densities. For comparison results are also presented for the binomial state, which gives a good description as well ( $\text{RMSD}/M'_s < 2\%$ ). Note that since the binomial distribution is closed under convolution,<sup>6,55</sup> the binomial parameter  $n$  (see Ref. 6) is in fact redundant: any subsystem size is described by a binomial distribution if the elementary system distribution is defined by a binomial or a convolution of binomial distributions. A two- or three-state binomial model ( $n = 1$  or  $2$ ) also provides a ratio  $N/\mathbb{N}$  of about 1. Interestingly, at  $55 \text{ mol/dm}^3$  the basic distributions of the models with  $N/\mathbb{N} \sim 0.85$  (beta and binomial models with  $n = 1$ ; see Fig. 7(A)) are very similar, with only two

discretelike polarization states. The basic distributions corresponding to models with  $N/\mathbb{N} \sim 1.35$  (discrete uniform and binomial models with  $n = 2$ ) are also rather similar, with three to four discrete polarization states. At  $45 \text{ mol/dm}^3$  we have a very similar situation.

From this we can conclude that, within the uncertainty of the “experimental” polarization data, the electric moment distribution of a water sample (at densities  $45.0$  and  $55.51 \text{ mol/dm}^3$  and at reference geometries  $^0f_d = 0.025$  and  $0.015$ , respectively) can be modeled by the convolution of a very large number of basic distributions, each describing approximately the behavior of one water molecule with two to four discretelike polarization states. These few discretelike polarization states are likely to be connected with the strongly directional hydrogen bonding network in water, which favors only some orientations per water molecule with respect to the external field. Note that the fact that each basic distribution describes approximately one water molecule does not necessarily imply that each water molecule in the system is statistically independent from the other ones; it only implies that in each independent (thermodynamic) subsystem, used to decompose the overall macroscopic distribution and to define the intensive thermodynamic properties, the distribution of the electric moment can be mathematically further decomposed into identical and independent “simple” distributions. When such basic distributions do not coincide with the fluctuation distributions of physically independent subsystems (which are never smaller than a single elementary system), they clearly cannot correspond to independent physical subparts of the system. In this case the basic distri-

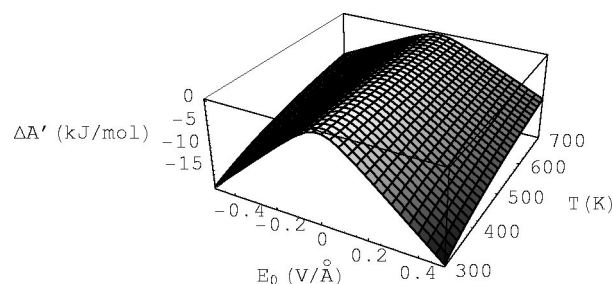


FIG. 8. Excess free energy  $\Delta A'(T, E_0)$  of water at  $\rho_N = 55.51 \text{ mol/dm}^3$  and  $^0f_d = 0.015$  as a function of temperature and external electric field, based on the gamma  $[U']$ +discrete uniform  $[M']$  EOS.

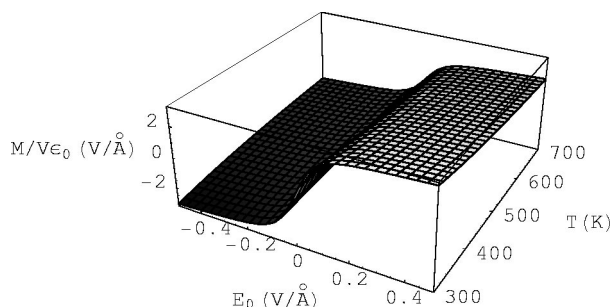


FIG. 9. Total electric moment  $M(T, E_0)$  of water at  $\rho_N = 55.51 \text{ mol/dm}^3$  and  $^0f_d = 0.015$  as a function of temperature and external electric field, based on the gamma  $[\mathcal{U}']$ +discrete uniform  $[\mathcal{M}']$  EOS.

butions simply provide via their convolution a mathematical model of the elementary system's distribution.

### C. Total EOS's

The best EOS, as a function of  $E_0$  and  $T$ , is for both densities given by a combination at  $T_0$  of the discrete uniform field model [Eqs. (49) and (50) with  $n=2$  and 3, respectively; see Table II] with the confined gamma state temperature model, the gamma  $[\mathcal{U}']$ +discrete uniform  $[\mathcal{M}']$  EOS. At  $55.51 \text{ mol/dm}^3$  we illustrate the behavior of this EOS via  $\Delta A'(T, E_0)$ ,  $M(T, E_0)$ ,  $\Delta S'(T, E_0)$ , and  $\Delta C'_V(T, E_0)$  at geometry  $f_d = ^0f_d = 0.015$  [Eqs. (34)–(37), (49), and (50)]; see Figs. 8–11. Note that the effect of the field on these thermodynamic properties is appreciable, especially on the heat capacity, considering that at 300 K and zero field  $A' = -23.9$ ,  $S' = -58.5$ , and  $C'_V = 48.7 \text{ J/mol K}$  (from the Saul–Wagner<sup>56</sup> water EOS). The effect of sample shape can be seen by (numerically) evaluating Eqs. (38)–(41) for  $f_d \neq ^0f_d$ ; however, the surfaces in  $T$  and  $E_0$  are very similar to Figs. 8–11 and are therefore not shown. In Figs. 12 and 13 we plot the predictions of  $\epsilon_r(T, E)$  from the gamma  $[\mathcal{U}']$ +discrete uniform  $[\mathcal{M}']$  EOS at  $45.0$  and  $55.51 \text{ mol/dm}^3$ , along with the (scaled) SPC/E data at  $T_0$  and experimental weak-field data for various isotherms. The EOS describes all available data very accurately. Unfortunately, it is difficult to check the behavior of the complete EOS because of the lack of additional “experimental” data, e.g., the field dependence for  $T > T_0$ .

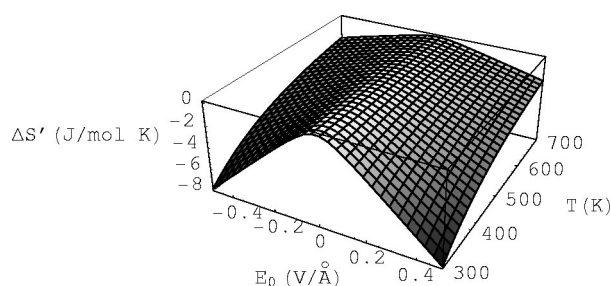


FIG. 10. Excess entropy  $\Delta S'(T, E_0)$  of water at  $\rho_N = 55.51 \text{ mol/dm}^3$  and  $^0f_d = 0.015$  as a function of temperature and external electric field, based on the gamma  $[\mathcal{U}']$ +discrete uniform  $[\mathcal{M}']$  EOS.

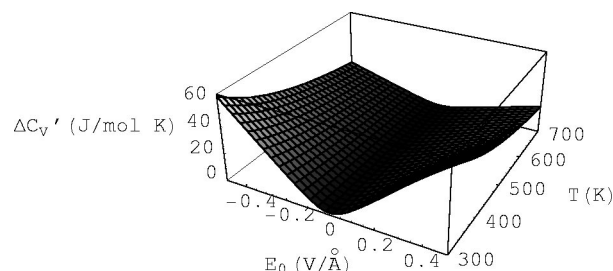


FIG. 11. Excess heat capacity  $\Delta C'_V(T, E_0)$  of water at  $\rho_N = 55.51 \text{ mol/dm}^3$  and  $^0f_d = 0.015$  as a function of temperature and external electric field, based on the gamma  $[\mathcal{U}']$ +discrete uniform  $[\mathcal{M}']$  EOS.

## IV. CONCLUSIONS

In this paper we extended the quasi-Gaussian entropy (QGE) theory in order to construct models providing the thermodynamic behavior of dielectric fluids as a function of temperature and electric field. This is achieved by combining a QGE model for energy fluctuations with a QGE model for fluctuations of the electromagnetic moment (as derived in the preceding paper). Results show that a specific “bivariate” EOS, the gamma  $[\mathcal{U}']$ +discrete uniform  $[\mathcal{M}']$  EOS, can describe the thermodynamics of polarized water within a wide range of temperature, density, and field. This EOS is based on the combination of a gamma state for the energy fluctuations (providing the temperature dependence) with a discrete uniform state for the electric moment fluctuations (providing the field dependence). The EOS is able to describe with high accuracy (1) the thermal behavior of the experimental weak-field dielectric constant of water at fixed density, ranging from dilute gas to dense liquid, and (2) the field dependence of water at fixed temperature for two liquid isochores ( $45.0$  and  $55.51 \text{ mol/dm}^3$ ) using a combination of experimental data and simulation data of the SPC/E water model.

Interestingly, in the field model the distribution of the macroscopic electric moment is constructed by the convolution of discrete uniform distributions, each describing ap-

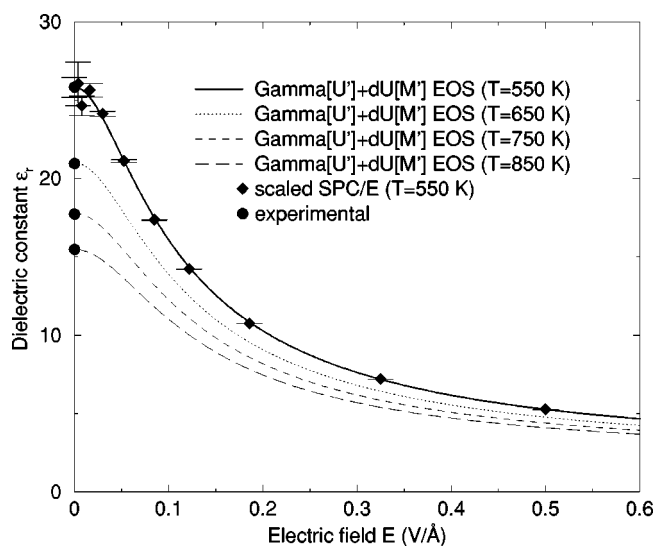


FIG. 12. Dielectric constant of water at  $\rho_N = 45.0 \text{ mol/dm}^3$  as a function of temperature and electric field: scaled SPC/E data, experimental weak-field data and gamma  $[\mathcal{U}']$ +discrete uniform  $[\mathcal{M}']$  EOS predictions.

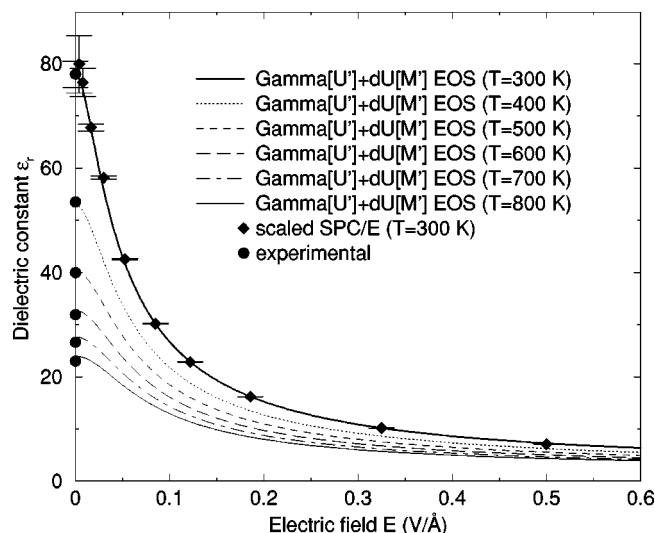


FIG. 13. Dielectric constant of water at  $\rho_N = 55.51 \text{ mol/dm}^3$  as a function of temperature and electric field: scaled SPC/E data, experimental weak-field data and gamma  $[U']$  + discrete uniform  $[M']$  EOS predictions.

proximately one water molecule with only a very limited set of possible polarization states (two to four). This is supported by the fact that for another accurate model, the beta state, the corresponding beta distribution is strongly U-shaped, implying only two discretelike polarization states. Such a result is probably due to the strong hydrogen bonding network of water molecules and implies that the electric moment distribution of each elementary system (which is the smallest physically independent thermodynamic subsystem) can be described by the convolution of a set of independent discrete uniform distributions.

It is also worth to remark that in our derivation the geometry of the sample becomes quite naturally a real state variable, with rather relevant effects in the liquid state. Note that the thermodynamics of dielectric fluids is very complex as it is dictated by the long-range molecular interactions and no simplifications based on a restricted available phase space can be used as in solids (such as cell theory and harmonic approximation). For this reason statistical mechanical calculations based on molecular Hamiltonian models are difficult, especially because of the polarization effects. A comparison between the QGE models and common mean-field models (the “ideal-gas” model, the polarizable and nonpolarizable Onsager models, and the Booth equation) shows that the physical trend for the first three models is acceptable. However, neither the weak-field limit nor the temperature and field dependence is correct. The Booth equation describes at 45.0 and 55.51 mol/dm<sup>3</sup> the field dependence rather well, although the weak-field limit and its thermal behavior are incorrect at all densities (gas to liquid). The use of fluctuation distribution models seems once again to be very useful and efficient in providing largely analytical EOS’s based on physical principles.

Finally, we expect that the combination of monovariate models to obtain multivariate EOS’s, as introduced in this paper, will be of great interest for modeling the thermody-

namic behavior as a function of many different state variables.

## ACKNOWLEDGMENTS

This research was supported by the Training and Mobility of Researchers (TMR) Program of the EU and The Dutch Technology Foundation STW. The hospitality of Professor Herman Berendsen and Professor Alan Mark during visits of MEFA to Groningen are greatly acknowledged, as well as stimulating discussions with Herman Berendsen.

## APPENDIX: EXPLICIT EXPRESSION OF $\mathcal{A}$

From the thermodynamic definition of the average electromagnetic moment in the direction of the field,  $M = -\partial\mathcal{A}/\partial\mathfrak{F}_0$  and Eqs. (1) or (2), we find

$$\left(\frac{\partial M}{\partial \mathfrak{F}_0}\right) = -\mathcal{A} + \beta\kappa_2[\mathcal{M}'], \quad (\text{A1})$$

with  $\kappa_2[\mathcal{M}'] = \langle(\mathcal{M}' - \langle\mathcal{M}'\rangle)^2\rangle$  the second central moment of  $\mathcal{M}'$ . From Eq. (1) of I we obtain that in the limit of zero field, where  $\partial M/\partial\mathfrak{F}_0 = M/\mathfrak{F}_0$ ,

$$\frac{V}{\zeta_0} \left( \frac{\chi}{1+f_d\chi} \right) = -\mathcal{A} + \beta\kappa_2[\mathcal{M}']. \quad (\text{A2})$$

The last equations can be used to obtain an explicit expression of  $\mathcal{A}$ . From Eq. (6), in the case where  $\langle\mathcal{M}'_i\rangle \equiv \langle\mathcal{M}'_0\rangle$ , i.e., the electromagnetic moment is basically independent of the bond quantum vibrational state. Assuming that at high temperature the system is still largely confined within the electronic ground state, although the exponential value in the integral of the partition function is virtually the unity because of the high temperature, we obtain that in such an “infinite” temperature limit the second central moment of  $\mathcal{M}'$  converges to a constant. Hence from Eq. (A1) it follows that  $\partial M/\partial\mathfrak{F}_0 = -\mathcal{A}$ . Using this result in the field derivative of Eq. (1) of I in the “infinite” temperature limit, we have

$$\frac{d\Omega}{d\mathfrak{F}_0} = -\frac{\Omega}{\mathfrak{F}_0} - \frac{\mathcal{A}}{\mathfrak{F}_0}, \quad (\text{A3})$$

where we defined for convenience  $\Omega = (V/\zeta_0)[\chi_\infty/(1+f_d\chi_\infty)]$  with  $\chi_\infty$  the “infinite” temperature limit of  $\chi$ . Equation (A3) is an ordinary linear differential equation with the general solution  $\Omega(\mathfrak{F}_0) = [\Omega(\mathfrak{F}_0^0) + \mathcal{A}](\mathfrak{F}_0^0/\mathfrak{F}_0) - \mathcal{A}$ , where  $\mathfrak{F}_0^0$  is the arbitrary initial field value used to solve the equation. In order to obtain the result that at “infinite” temperature the zero-field limit of  $\Omega$  converges to the value provided by Eq. (A2), we must set  $\Omega(\mathfrak{F}_0^0) = -\mathcal{A}$ , and so at any field

$$\mathcal{A} = -\frac{V}{\zeta_0} \left( \frac{\chi_\infty}{1+f_d\chi_\infty} \right), \quad (\text{A4})$$

meaning that  $\chi_\infty$  is independent of the field and that  $\mathcal{A}$  is, in contrast to  $\chi$ , in general dependent on the geometry of the system. Moreover, from Eq. (A2) we have

$$\beta\kappa_2[\mathcal{M}'] = \frac{V}{\zeta_0} \frac{\chi - \chi_\infty}{(1+f_d\chi)(1+f_d\chi_\infty)}. \quad (\text{A5})$$

- <sup>1</sup>A. Amadei, M. E. F. Apol, and H. J. C. Berendsen, *J. Chem. Phys.* **106**, 1893 (1997).
- <sup>2</sup>A. Amadei, M. E. F. Apol, and H. J. C. Berendsen, *J. Chem. Phys.* **109**, 3004 (1998).
- <sup>3</sup>M. E. F. Apol, A. Amadei, H. J. C. Berendsen, and A. Di Nola, *J. Chem. Phys.* **111**, 4431 (1999).
- <sup>4</sup>M. E. F. Apol, A. Amadei, H. J. C. Berendsen, and A. Di Nola (unpublished).
- <sup>5</sup>M. E. F. Apol, A. Amadei, and H. J. C. Berendsen, *J. Chem. Phys.* **109**, 3017 (1998).
- <sup>6</sup>M. E. F. Apol, A. Amadei, and A. Di Nola, *J. Chem. Phys.* **116**, 4426 (2002), preceding paper.
- <sup>7</sup>D. Roccatano, A. Amadei, M. E. F. Apol, A. Di Nola, and H. J. C. Berendsen, *J. Chem. Phys.* **109**, 6358 (1998).
- <sup>8</sup>A. Amadei, M. E. F. Apol, G. Chillemi, H. J. C. Berendsen, and A. Di Nola, *Mol. Phys.* **96**, 1469 (1999).
- <sup>9</sup>A. Amadei, G. Chillemi, M. A. Ceruso, A. Grottesi, and A. Di Nola, *J. Chem. Phys.* **112**, 9 (2000).
- <sup>10</sup>L. D. Landau and E. M. Lifshitz, *Statistical Physics, Part 1*, 3rd ed. (Pergamon, Oxford, 1980).
- <sup>11</sup>L. D. Landau and E. M. Lifshitz, *Statistical Physics, Part 2*, 3rd ed. (Pergamon, Oxford, 1980).
- <sup>12</sup>Note that the classical potential energy and the mass tensors for a given configuration, as well as the integration limits, are in principle different for different quantum vibrational states. However, in Eq. (2) such differences can be in general safely neglected. It should be also noted that at zero field, Eq. (2) reduces to the usual expression [Eqs. (2) and (3) of Ref. 1], valid for semirigid molecules, if  $\Pi_{j=1}^N (\det \bar{M}_j)^{1/2}$  is constant over the configurations. Hence the integral over the momenta can be considered independent of the coordinates, although the integrand generally is not. In that case the partition function can be factorized into two independent integrals: one over the coordinates involving the potential energy and another over the momenta involving the kinetic energy (Refs. 1, 10, and 11).
- <sup>13</sup>N. I. Johnson, S. Kotz, and A. W. Kemp, *Univariate Discrete Distributions*, 2nd ed. (Wiley, New York, 1992).
- <sup>14</sup>A. Stuart and J. K. Ord, *Kendall's Advanced Theory of Statistics*, 5th ed. (Griffin, London, 1987), Vol. 1.
- <sup>15</sup>M. Aschi, R. Spezia, A. Di Nola, and A. Amadei, *Chem. Phys. Lett.* **344**, 374 (2001).
- <sup>16</sup>M. Raynaud, C. Reynaud, Y. Ellinger, G. Hennico, and J. Delhalle, *Chem. Phys.* **142**, 191 (1990).
- <sup>17</sup>C. Kittel, *Introduction to Solid State Physics*, 5th ed. (Wiley, New York, 1976).
- <sup>18</sup>B. I. Bleaney and B. Bleaney, *Electricity and Magnetism*, 3rd ed. (Oxford University Press, Oxford, 1976).
- <sup>19</sup>P. W. Selwood, *Magnetochemistry*, 2nd ed. (Interscience, New York, 1956).
- <sup>20</sup>K.-H. Hellwege, *Einführung in die Festkörperphysik* (Springer-Verlag, Berlin, 1976).
- <sup>21</sup>Note that a more general Gaussian [ $\mathcal{U}$ ] + Gaussian [ $\mathcal{M}$ ] expression of  $\chi^0(T)$ , treating also the effect of sample shape, is given by Eq. (46) where in that case  $z(T) = T_0/T$ .
- <sup>22</sup>H. J. C. Berendsen, J. R. Grigera, and T. P. Straatsma, *J. Phys. Chem.* **91**, 6269 (1987).
- <sup>23</sup>D. P. Fernández, A. R. H. Goodwin, E. W. Lemmon, J. M. H. Levelt Sengers, and R. C. Williams, *J. Phys. Chem. Ref. Data* **26**, 1125 (1997).
- <sup>24</sup>W. Wagner and A. Kruse, *Properties of Water and Steam* (Springer-Verlag, Berlin, 1998).
- <sup>25</sup>D. P. Fernández, Y. Mulev, A. R. H. Goodwin, and J. M. H. Levelt Sengers, *J. Phys. Chem. Ref. Data* **24**, 33 (1995).
- <sup>26</sup>A. Amadei, Ph.D. thesis, Rijksuniversiteit Groningen, The Netherlands, 1998. Also available from <http://docserv.ub.rug.nl/eldoc/dis/science/a.amadei/>
- <sup>27</sup>P. Schiebener, J. Straub, J. M. H. Levelt Sengers, and J. S. Gallagher, *J. Phys. Chem. Ref. Data* **19**, 677 (1990).
- <sup>28</sup>P. Schiebener, J. Straub, J. M. H. Levelt Sengers, and J. S. Gallagher, *J. Phys. Chem. Ref. Data* **19**, 1617 (1990).
- <sup>29</sup>F. Booth, *J. Chem. Phys.* **19**, 391 (1951).
- <sup>30</sup>F. Booth, *J. Chem. Phys.* **19**, 1327 (1951).
- <sup>31</sup>F. Booth, *J. Chem. Phys.* **19**, 1615 (1951).
- <sup>32</sup>H. A. Kolodziej, G. Parry Jones, and M. Davies, *J. Chem. Soc., Faraday Trans. 2* **71**, 269 (1975).
- <sup>33</sup>Y. Marcus, *The Properties of Solvents* (Wiley, New York, 1998).
- <sup>34</sup>Y. Marcus and G. Hefter, *J. Solution Chem.* **28**, 575 (1999).
- <sup>35</sup>I.-C. Yeh and M. L. Berkowitz, *J. Chem. Phys.* **110**, 7935 (1999).
- <sup>36</sup>D. van der Spoel, P. J. van Maaren, and H. J. C. Berendsen, *J. Chem. Phys.* **108**, 10220 (1998).
- <sup>37</sup>S.-B. Zhu, S. Sing, and G. W. Robinson, *Adv. Chem. Phys.* **85**, 627 (1994).
- <sup>38</sup>T. Darden, D. York, and L. Pedersen, *J. Chem. Phys.* **98**, 10089 (1993).
- <sup>39</sup>U. Essmann, L. Perera, M. L. Berkowitz, T. Darden, H. Lee, and L. G. Pederson, *J. Chem. Phys.* **103**, 8577 (1995).
- <sup>40</sup>S. W. de Leeuw, J. W. Perram, and E. R. Smith, *Proc. R. Soc. London, Ser. A* **373**, 27 (1980).
- <sup>41</sup>M. Neumann, *Mol. Phys.* **50**, 841 (1983).
- <sup>42</sup>H. J. C. Berendsen, D. van der Spoel, and R. van Drunen, *Comput. Phys. Commun.* **91**, 43 (1995).
- <sup>43</sup>E. Lindahl, B. Hess, and D. van der Spoel, *J. Mol. Model.* [Electronic Publication] **7**, 306 (2001).
- <sup>44</sup>D. van der Spoel, A. R. van Buuren, E. Apol *et al.*, *Gromacs User Manual Version 3.0* (Nijenborgh, Groningen, The Netherlands, 2001). Internet: <http://www.gromacs.org>
- <sup>45</sup>H. J. C. Berendsen, J. P. M. Postma, W. F. van Gunsteren, A. Di Nola, and J. R. Haak, *J. Chem. Phys.* **81**, 3684 (1984).
- <sup>46</sup>D. J. Evans and G. P. Morris, *Comput. Phys. Rep.* **1**, 297 (1984).
- <sup>47</sup>T. Morishita, *J. Chem. Phys.* **113**, 2976 (2000).
- <sup>48</sup>S. Miyamoto and P. A. Kollman, *J. Comput. Chem.* **13**, 952 (1992).
- <sup>49</sup>M. P. Allen and D. J. Tildesley, *Computer Simulation of Liquids* (Oxford University Press, Oxford, 1989).
- <sup>50</sup>T. P. Straatsma, H. J. C. Berendsen, and A. J. Stam, *Mol. Phys.* **57**, 89 (1986).
- <sup>51</sup>M. Bishop and S. Frinks, *J. Phys. Chem.* **87**, 3675 (1987).
- <sup>52</sup>I. M. Svishchev and P. G. Kusalik, *J. Phys. Chem.* **98**, 728 (1994).
- <sup>53</sup>L. Onsager, *J. Am. Chem. Soc.* **58**, 1486 (1936).
- <sup>54</sup>D. C. Grahame, *J. Chem. Phys.* **21**, 1054 (1953).
- <sup>55</sup>W. Feller, *An Introduction to Probability Theory and Its Application*, 3rd ed. (Wiley, New York, 1968), Vol. 1.
- <sup>56</sup>A. Saul and W. Wagner, *J. Phys. Chem. Ref. Data* **18**, 1537 (1989).